Improved Drosophila Visual Neural Network Application in Vehicle Target Tracking and Collision Warning

Jianyi Wu
School of Traffic Management and Engineering, Guangxi Police College, Nanning 530023, China

***Abstract*—To enable the vehicle tracking and collision warning system to face more complex road information, the Drosophila visual neural network collision warning algorithm has been improved, including image stabilization algorithm, target region synthesis algorithm, and target tracking algorithm. The results showed that the improved image stabilization algorithm had significantly higher image stabilization quality. The peak signal-to-noise ratio of the stabilized image before improvement was the highest at 80dB and the lowest at 54dB. After improvement, the peak signal-to-noise ratio of the stabilized image was the highest at 82dB and the lowest at 60dB. The improved algorithm did not have any false alarms or missed alarms in collision warning. In video 1, there were false alarms in the unimproved algorithm, while in video 2, there were missed alarms. In video 1, all frames were in a safe state, but the original algorithm displayed an alarm in frames 7-12, 13-22, and 23-31. In video 2, there were dangerous situations in frames 8-24 that required an alarm, while the original algorithm displayed an alarm message in frames 8-17, consistent with the actual situation. The improved target tracking algorithm can complete the task of extracting target motion curves. The target tracking algorithm extracted the motion curves of one target in video 1 and two targets in video 2, which were consistent with the video content. The improvement of the Drosophila visual neural network collision warning model through research is effective, which can improve the driving safety of vehicles in complex road conditions.**

Keywords*—Drosophila visual neural network; collision warning; target calibration; target tracking

I. Introduction

With the continuous development of the social economy and the continuous improvement of people's travel standards, the number of private cars has reached 402 million. However, with the continuous growth of the number of motor vehicles, the incidence of traffic accidents is also increasing, with traffic accidents accounting for over 80% of all safety accidents [1]. The occurrence of traffic accidents not only causes huge economic losses, but also seriously threatens people's life safety. In large-scale traffic accidents, the survival rate of personnel is basically 0. The lack of concentration among drivers is the main cause of traffic accidents. If a warning system can be designed to provide early warning for drivers, increase their reaction time, and prevent accidents before they occur, it can fundamentally solve traffic safety accidents. This not only protects personal safety, but also avoids economic losses. Therefore, designing an active safety system for vehicles has become the main research direction of scholars [2]. The driver's information perception mainly relies on visual perception, but human vision has limitations. Some insects, if flies have comprehensive vision, can obtain more driving information. Therefore, we propose to use an improved fruit fly visual neural network for vehicle target tracking and collision warning, providing drivers with more driving information and ensuring safety beside the vehicle.

The study first proposed and applied an improved Drosophila visual neural network for vehicle target tracking and collision warning. This new application fully utilizes the comprehensive view of fruit flies, providing drivers with more driving information, thereby significantly improving the driving safety of the vehicle. And the innovative integrated early warning function can increase the driver's reaction time and even prevent accidents before they occur. This feature will directly reduce the occurrence of large-scale traffic accidents, protect personal safety, and avoid economic losses.

The first part is a review of the current research status of foreign vehicle collision warning and Drosophila visual neural network. The second part is the application research of improved Drosophila visual neural network in vehicle tracking and collision warning. The third part is the analysis of experimental simulation results of model application. The fourth part summarizes the research content and points out the shortcomings, and clarifies the future development direction.

II. Related Works

Effective vehicle tracking and collision warning system can help drivers avoid many traffic safety accidents. Sanberg et al. believed that the current collision warning system was based on radar system and monocular vision, with more redundancy. To reduce the redundancy of the system, a collision warning system based on stereo vision was proposed, which can detect obstacles on the vehicle path without relying on Semantic information. The final evaluation results indicated that when the obstacle was higher than 0.4m, all obstacles in the dataset can be detected [3]. To solve the anti-collision problem in autonomous vehicle, Hu et al. developed a path planning and tracking framework based on model predictive control. This framework not only considered the friction coefficient between the tire and the road, but also considered the lateral distance control of the vehicle and the adaptive weight of the speed output in various situations. The anti-collision experiment results showed that the framework developed by the author had practical significance. It can cope

with the anti-collision task of the current auto drive system [4]. To reduce the collision probability of autonomous vehicles, Cao and Jiang designed a trajectory planning and tracking control method for formation driving. The trajectory planning of this method was divided into two stages: stable speed tracking and parameter matching. The results showed that this method can effectively avoid static and dynamic obstacles, and compared with traditional controllers, this method had higher stability and more accurate tracking [5]. Zhou et al. designed a trajectory planning and tracking control strategy in order to achieve the safe driving of the driverless vehicle to the destination. This strategy uses the artificial fish school algorithm to plan the optimal path from the starting point to the end point, and uses the forward search algorithm based on Markov chain to plan the path in the local path with obstacles. The simulation results show that, the trajectory planning and control strategy proposed by the author is sufficient to face static obstacles and some dynamic obstacles [6].

Tokuda proposed a visual servo scheme based on convolutional neural networks to make the positioning of the robotic arm more accurate. In this scheme, the eye and hand cameras were used to capture the desired image and the current image to estimate the relative pose between the desired end effector and the current end effector. Simulation results showed the effectiveness of this method [7]. Burguera et al. proposed an architecture based on an automatic encoder for the rapid and stable visual loop detection of underwater robots. The decoder part of this architecture was replaced by a fully connected layer. The results showed that this neural network can improve the visual loop detection efficiency of underwater robots [8]. Gu et al. proposed a novel convolutional neural network architecture for visual availability detection in the fields of robotics and computer vision. The architecture adopted an encoder decoder architecture for acute pixel level availability detection, where the encoder network included residual modules and multi-level dependent attention mechanisms. The experimental results showed that this method improved the performance of the neural network in the attention mechanism and sampling layer networks, laying the foundation for the research on multi task learning of physical robots [9]. To solve the problem of collision perception between robots and autonomous vehicle, Q Fu et al. constructed a visual neural network based on a lobular giant motion detector. The construction of the network referred to the visual path of locusts. In the simulation experiment, the method passed the system test of real scene stimulation, indicating that the model can effectively detect hidden obstacles under various dynamic and chaotic backgrounds [10].

In summary, the main safety issue faced by autonomous vehicle systems is the collision problem during vehicle operation. Efficient and accurate collision warning can effectively improve the safety of vehicle operation. Collision warning is based on visual detection of obstacles to avoid, and visual neural networks can effectively detect obstacle information in images to achieve vehicle collision warning.

III. Vehicle Tracking Collision Warning Based on Improved Drosophila Visual Neural Network

The main content of this chapter is to design and construct a vehicle tracking collision warning model and a target tracking and vehicle collision detection model, which is divided into two sections. The first section is the establishment of a collision detection model based on an improved Drosophila visual neural network, and the second section is the construction of a target tracking and vehicle collision warning model.

A. Collision Detection Model Based on Improved Drosophila Visual Neural Network

During the driving process of vehicles, due to obstacles or unevenness on the road surface, there may be shaking and other phenomena, resulting in missing or unreadable information recorded by the onboard camera. Therefore, the study proposes to divide the image area equally, improve the grayscale projection image stabilization algorithm, and use the improved algorithm to complete the distorted image or video [11-12]. The grayscale projection algorithm can use the grayscale value of the reference frame to complete the motion vector of the current frame, obtain a stable image sequence, study dividing the image into sub grids of equal size, and then use the grayscale algorithm to calculate the motion vector of the target within each sub grid. After integrating the motion vectors within each sub grid, the overall motion vector of the image can be obtained. The overall motion vector estimation algorithm process is shown in Fig. 1.

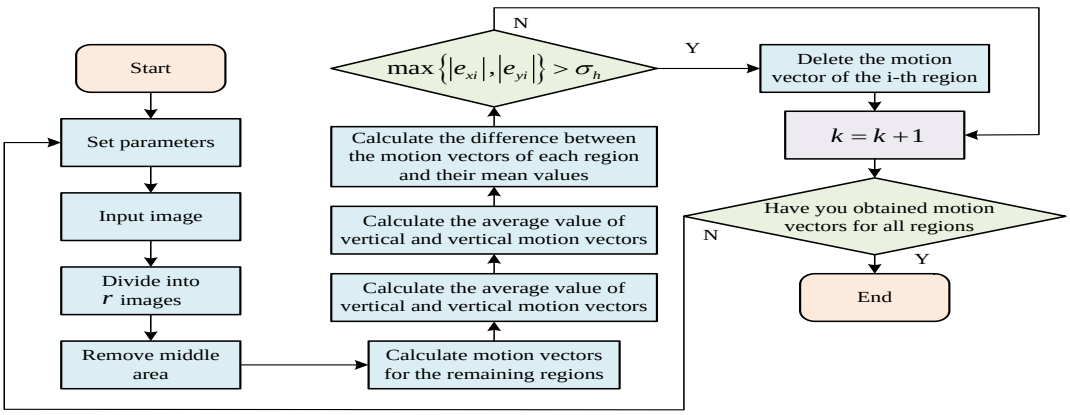

Fig. 1. Global motion vector estimation algorithm.

The threshold of the algorithm is set to σ_h, $k=1$. The image is input into the algorithm. The lower 75% of the image is divided into r small cells of the same size, the motion vectors of the small cells are calculated except for the middle region, and the set of motion vectors is obtained in the horizontal and vertical directions of the region block, as shown in formula (1).

$$\begin{cases} V_x = \{v_{x1}, v_{x1}, \ldots, v_{x,r-1}\} \\ V_y = \{v_{y1}, v_y, \ldots, v_{y,r-1}\} \end{cases} \tag{1}$$

In formula (1), V_x, V_y represent the sum of motion vectors in the horizontal and vertical directions, and v_{x1}, v_{y1} represent the motion vectors in the horizontal and vertical directions of region 1. After obtaining the motion vectors in the horizontal and vertical directions for all regions except the central region, the average value v_{ax}, v_{ay} of the motion vectors is calculated in the horizontal and vertical directions, and then calculate the deviation value e_{xi} between v_x, v_y and v_{ax}, v_{ay} for each region, to determine whether the deviation value meets formula (2).

$$\max\left\{|e_{xi}|, |e_{yi}|\right\} > \sigma_h \tag{2}$$

If satisfied, the motion vectors of each region i in V_x, V_y are deleted, where V_x, V_y is the global motion vector of the image, $k=k+1$. The global motion vector is calculated for the next frame until the global motion vector for each frame is obtained. The above algorithm can obtain the superposition of motion vectors generated by normal shooting or shaking shooting of car mounted cameras [13-14]. The purpose of the image stabilization algorithm is to preserve the motion information obtained by the camera during normal shooting and eliminate information loss caused by shaking shooting. Therefore, a new image stabilization algorithm has been studied and designed, and its process is shown in Fig. 2.

After determining the memory scale U, maximum offset T_1, cumulative offset $M=0$, and other parameters of the algorithm, the stable image is output. Then the global motion vector estimation algorithm is used to calculate the global motion vector v_{xi}, v_{yi} of frame i relative to frame $i-1$, $k=k+1$. The grayscale of frame k is input, the global motion vector v_{xk}, v_{yk} of frame k relative to frame $k-1$ is calculated, and then the average motion vector $\bar{v}_{xk}, \bar{v}_{yk}$ in the horizontal and vertical directions of the adjacent L-frame grayscale before frame k is calculated. The cumulative offset M of two frames of images is calculated using formula (3).

$$M = M + \sqrt{\Delta v_{xk}^2 + \Delta v_{yk}^2} \tag{3}$$

In formula (3), $\Delta v_{xk}^2, \Delta v_{yk}^2$ represents the difference between the motion vectors of two grayscale images. At this point, if $M < T_1$, the motion vector Δ_{xk}, Δ_{yk} will be compensated for the corresponding distance in the opposite direction, and the image in frame k will be compensated and replaced. Then, $k=k+1$ will start a new round of calculation until $M \geq T_1$, and if $M \geq T_1$, the motion vector $\left[\Delta_{xk}, \Delta_{yk}\right]$ will be compensated for the corresponding pixel distance in the opposite direction to compensate for the image in frame k. Let $k=k+1$, $M=0$ start motion compensation for the next grayscale image again until all images have completed stabilization. In addition to the stability of moving images, collision detection algorithms also need to consider the influence of weather factors. Traditional weather recognition algorithms are difficult to meet the needs of weather recognition in complex environments. Therefore, research has proposed adding parameters to improve the weather recognition algorithm. Firstly, the study has added standard deviation parameters, which can reflect the degree of image dispersion. The larger the standard deviation, the smaller the impact on image target extraction, the calculation of standard deviation is shown in formula (4).

$$\sigma = \sqrt{\sum_{i=0}^{L-1} \left(z_i - m\right)^2 p\left(z_i\right)} \tag{4}$$

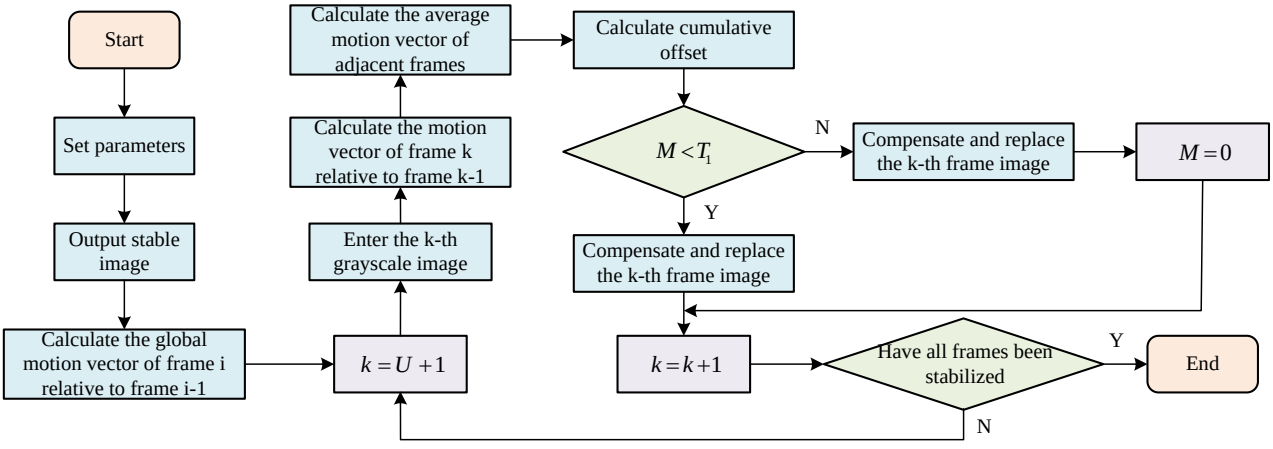

Fig. 2. Image stabilization algorithm flow.

In formula (4), σ represents the standard deviation, L represents the total number of grayscale levels, z_i represents the i-th grayscale level, $p(z_i)$ represents the probability of grayscale being z_i in the grayscale distribution of the histogram, and m is the pixel mean. Secondly, the study adds a smoothness parameter, which is an important characteristic of image texture. The higher the smoothness, the worse is the image smoothness. The calculation of smoothness is shown in formula (5).

$$R = \frac{1}{1+\sigma^2} \tag{5}$$

In formula (5), R represents smoothness. Finally, the study also adds image entropy, which can reflect the degree of similarity between different images. The calculation of image entropy is shown in formula (6).

$$e = -\sum_{i=0}^{L-1} p(z_i)\log_2 p(z_i) \tag{6}$$

In formula (6), e represents image entropy. After introducing the above three parameters, the indicators for measuring sunny days are shown in formula (7).

$$w_1^{'} = a_{10}B + a_{11}A + a_{12}C + a_{13}p_r + a_{14}\sigma + a_{15}R + a_{16}e \tag{7}$$

In formula (7), $w_1^{'}$ represents the sunny day metric, a_{ij} represents the weighting coefficient, A represents the image sharpness, B represents the image brightness, C represents the image contrast, and p_r represents the proportion of image value neighborhoods. The formula for measuring indicators on cloudy days is shown in formula (8).

$$w_2^{'} = a_{20}(1-B) + a_{21}A + a_{22}C + a_{23}(1-p_r) + a_{24}\sigma + a_{25}R + a_{26}e \tag{8}$$

In formula (8), $w_2^{'}$ represents that in addition to cloudy and sunny days, the measurement index for cloudy days also needs to consider foggy days. The measurement index formula for foggy days is shown in formula (9).

$$w_3^{'} = a_{30}(1-B) + a_{31}(1-A) + a_{32}(1-C) + a_{33}p_r + a_{34}(1-\sigma) + a_{35}R + a_{36}e \tag{9}$$

In formula (9), $w_3^{'}$ represents the measurement indicator for foggy weather. By replacing the indicators in traditional weather recognition algorithms with the above three measurement indicators, an improved weather recognition algorithm can be obtained. The Drosophila visual neural network can detect moving targets, but it is limited to the direction detection of moving targets. After scholars' improvement, the Drosophila visual neural network can perform collision detection of moving targets. The photosensitive cell layer of the visual neural network that can perform collision detection has $I \times J$ photosensitive cells, corresponding to the grayscale value of the grayscale image of size $I \times J$, so that $L_{ij}(t)$ represents (i, j) grayscale value at time t, The output of photosensitive cell (i, j) at time t can be expressed using formula (10).

$$P_{ij}(t) = \frac{1}{2}\left(L_{ij} + f\left(L_{ij}\right)\right), 1 \le i \le I, 1 \le j \le J \tag{10}$$

In formula (10), $P_{ij}(t)$ represents the output of the photosensitive cell at time t, and $f(\square)$ represents the time delay function. After combining the improved image processing technology with a visual neural network with collision detection function, an improved Drosophila visual neural network algorithm can be obtained. The algorithm process is shown in Fig. 3.

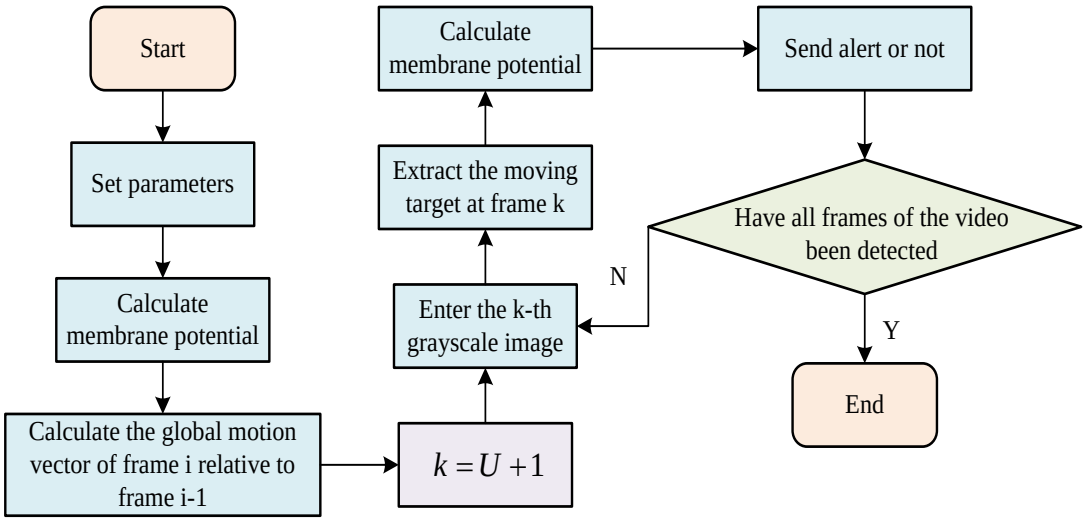

Fig. 3. Improved Drosophila visual neural network collision detection algorithm.

Initial parameters are input, neural network is used to obtain membrane potential $Y_{lob}(0),\ldots,Y_{lob}(U)$, and global motion vector is calculated, $k=U+1$. Grayscale image of frame k is input to extract foreground moving targets and neural network is used to obtain membrane potential $Y_{lob}(k)$. If $Y_{lob}(k)$ is greater than collision warning threshold, warning signal will be sent, $k \leftarrow k+1$. Foreground moving targets are extracted in the next frame and membrane potential. Whether warning is needed is determined until each frame of the video completes detection [15-16].

B. Construction of Target Tracking and Vehicle Collision Warning Model

In the binary image of a video, there may be a phenomenon where moving targets are divided into multiple interconnected regions, which affects the recognition of the number of moving targets in the field of view and leads to target tracking failure. Therefore, the study first uses corrosion and dilation algorithms to process the binary image, then calibrates the moving targets in the binary image, records the center point position of the targets, and finally uses region synthesis algorithms to determine the number of moving targets in the image. In a binary graph, different connected regions of the same moving target can be merged using the distance between the bounding rectangles of the moving target area and the distance threshold. The distance between the bounding rectangles is calculated using formula (11).

$$d(L_a,L_b)=\sqrt{d_h^2+d_v^2} \tag{11}$$

In formula (11), $d(L_a,L_b)$ represents the distance between region a and region b, and d_h, d_v represent the horizontal width distance and vertical height distance of region a,b. The calculation of d_h is shown in formula (12).

$$d_h=\begin{cases}0, & d_h^{ab}\le\frac{1}{2}(h_a+h_b)\\ d_h^{ab}-\frac{1}{2}(h_a+h_b), & d_h^{ab}>\frac{1}{2}(h_a+h_b)\end{cases} \tag{12}$$

In formula (12), d_h^{ab} represents the horizontal projection distance between the center points of the bounding rectangle in the target area, and h_a, h_b represent the horizontal height of the target area. The calculation of d_v is shown in formula (13).

$$d_v=\begin{cases}0, & d_v^{ab}\le\frac{1}{2}(h_a+h_b)\\ d_v^{ab}-\frac{1}{2}(v_a+v_b), & d_v^{ab}>\frac{1}{2}(h_a+h_b)\end{cases} \tag{13}$$

In formula (13), d_v^{ab} represents the vertical projection distance between the center points of the bounding rectangle in the target area, and v_a, v_b represents the vertical distance of the target area. The target region synthesis algorithm designed for research is shown in Fig. 4.

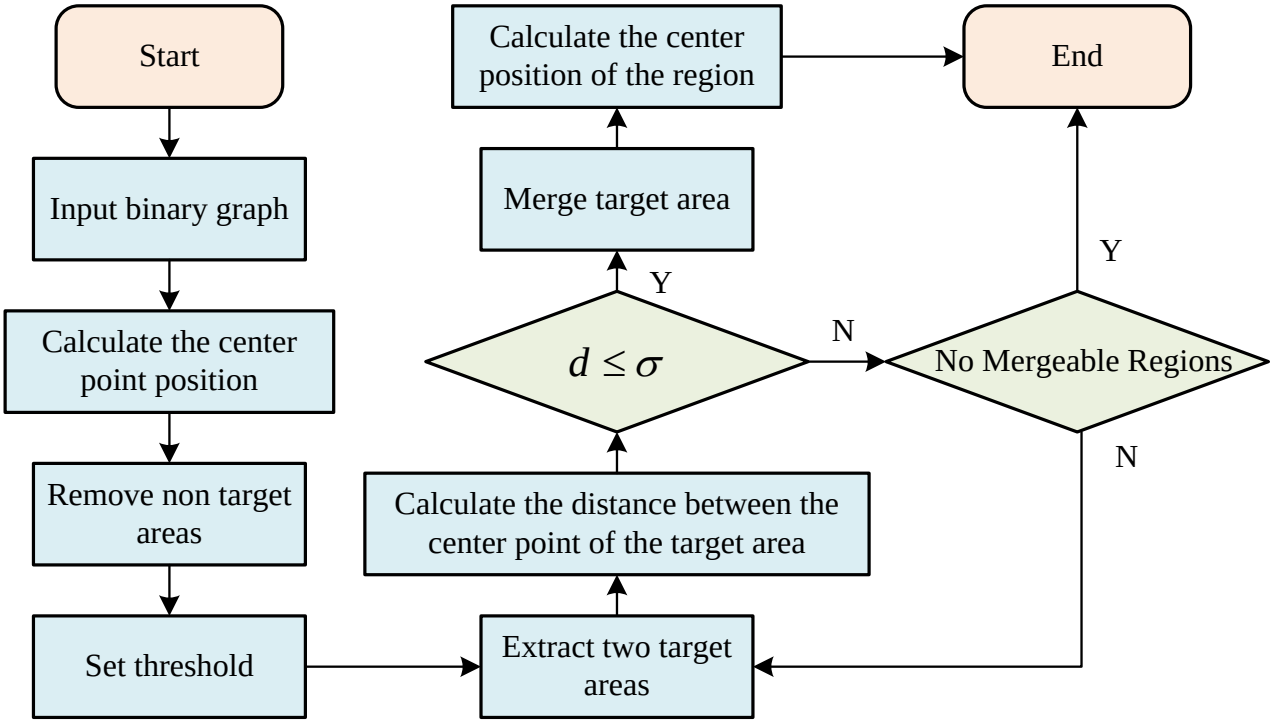

Fig. 4. Target region synthesis algorithm flow.

After inputting the binary image, the synthesized moving target in the target area is output. Through target calibration, the center point positions of the outer rectangles of each connected area are obtained. Then, by eliminating the target area, a binary image containing only the target area is obtained. If n represents the number of target areas, the target area is aggregated as $L=\{l_1 l_2,\ldots,l_n\}$, and the distance threshold is set as σ. The distance between adjacent target areas is calculated using formula (11), If the distance between two adjacent target areas is less than or equal to σ, the two target areas will be merged and the center point coordinates of the merged target area will be recalculated. If it is greater than σ, adjacent target areas will be re selected to determine whether to merge until all adjacent target areas have a distance greater than σ. In this algorithm, the center position of the target area can be determined, so the motion speed of the same moving target in adjacent frame images can be calculated using formula (14).

$$v=\sqrt{\left(x_{1j\_ctr}-x_{2j\_ctr}\right)^2+\left(y_{1j\_ctr}-y_{2j\_ctr}\right)} \tag{14}$$

In formula (14), $\left(x_{1j\_ctr},y_{1j\_ctr}\right)$ and $\left(x_{2j\_ctr},y_{2j\_ctr}\right)$ represent the center position of the j-th moving target in adjacent images [17-18]. The target tracking algorithm is not only related to the position and speed of the target, but also to changes in the environment. Therefore, a new target tracking algorithm has been studied and designed, and its process is shown in Fig. 5.

After inputting the initial parameter attribute set *object*, an image sequence of size $I\times J$ is output. The image frame counter is set to 0, various parameters of *object* are initialized, and then the number of targets is reset. $k=l+1$, the target region synthesis algorithm and formula (14) are used to calculate the positions and motion velocities of all targets in frame k. If the image frame counter is 0, the position and velocity of targets in frame *object* are updated. If it is greater than 0, the position of targets in frame *object* is used to predict the position of targets in frame k. Then, formula (15) is used to calculate the distance d between the target position and the predicted position.

$$d=\sqrt{\left(x_0-x_m\right)^2+\left(y_0-y_m\right)^2} \tag{15}$$

In formula (15), x_0,y_0 represents the predicted position and x_m,y_m represents the calculated position. At this point, if d is less than the threshold, the target in *object* matches the target in frame k of the image. The target position in *object* is updated using the target position in the image until the image target leaves the visual area and all frames of the video image have been detected. This algorithm has improved the input parameter quality of the neural network, but has not improved the neural network and warning scheme. Therefore, the model is only suitable for a single moving target and cannot detect the motion direction of multiple targets. Thus, a new object tracking and collision warning algorithm has been studied and designed, and its process is shown in Fig. 6.

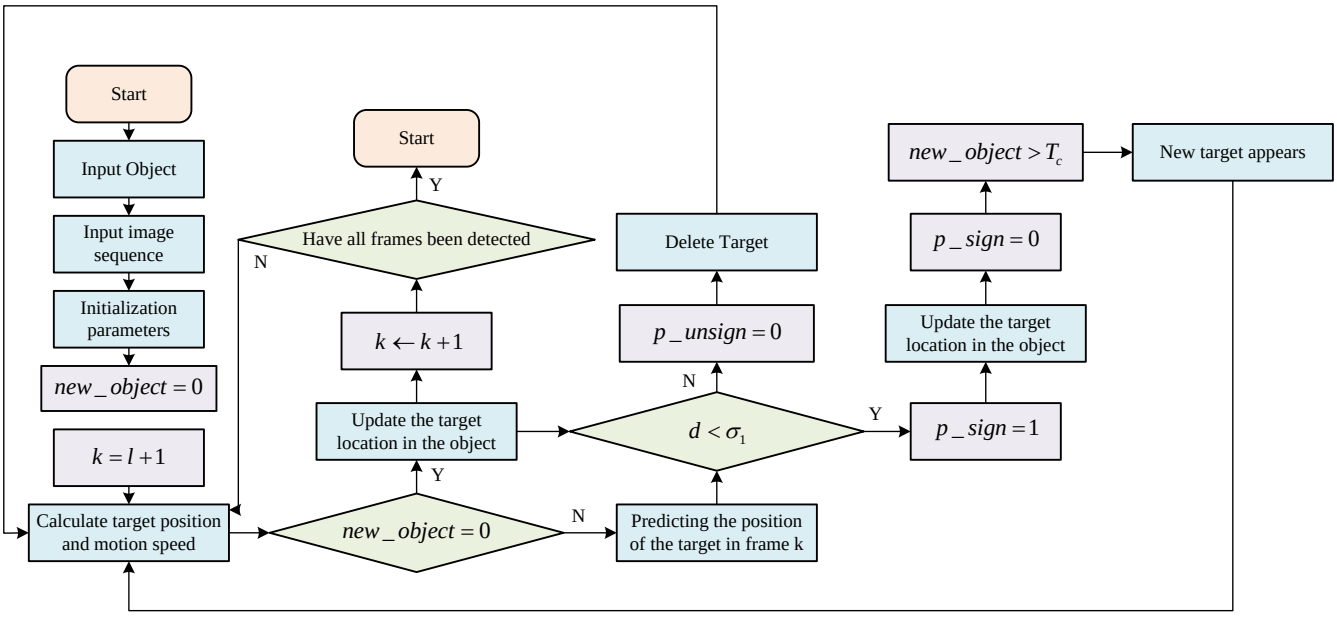

Fig. 5. Target tracking algorithm flow.

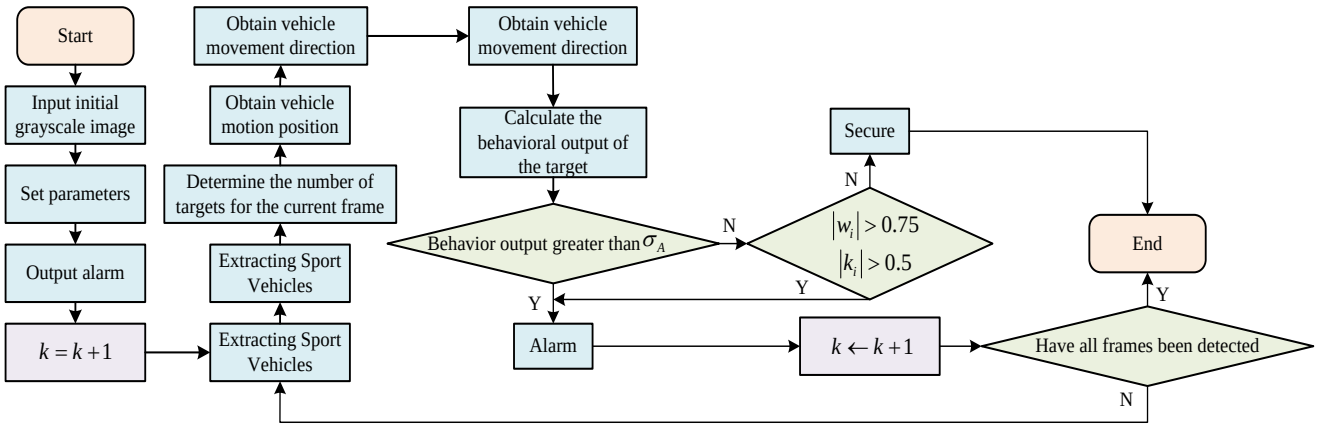

Fig. 6. Target tracking and collision warning algorithm flow.

An initial grayscale image of size $I \times J$ is input, the dynamic threshold σ_A and warning threshold frame number T of the algorithm are set, the warning signal is output. $k=l+1$, the grayscale image of frame k is input, and the moving target of the image is extracted. The target area synthesis algorithm is used to determine the number of moving targets in the image, and then the target tracking algorithm is used to obtain the vehicle's motion position and direction. After obtaining the motion information of the target in the image, an artificial Drosophila visual neural network is used to calculate the behavior output of a vehicle, if the behavior output of the vehicle is greater than σ_A, a warning will be issued. If the behavior output of the vehicle is less than σ_A, the slope of the moving vehicle's motion direction will be calculated. If the absolute value of the moving vehicle's position is greater than 0.75, and the absolute value of the slope is greater than 0.5, a warning signal will be sent. Finally, $k \leftarrow k+1$, the behavior output of the vehicle can be obtained and compared with σ_A until all image frames are detected.

IV. Simulation Experimental Results

This Section is an experimental validation analysis of the content of Section II, divided into two sections. The first section is the experimental validation analysis of improving the Drosophila visual neural network collision detection model, and the second section is the experimental validation analysis of target tracking and vehicle collision warning algorithms. The experimental validation analysis of improving the collision detection model of the Drosophila visual neural network can verify the recognition accuracy of the proposed algorithm in different situations, and the experimental validation analysis of target tracking and vehicle collision warning algorithms can verify whether the algorithm proposed by the acting team is effective in protecting drivers and personnel.

A. Collision Warning Experiment

To verify the feasibility of improving the Drosophila visual neural network collision model through research, experimental research was conducted under the OpenC V2.4.9 configuration in the Visual Studio 2010 software of the Windows 7 system. The study compared the Peak Signal to Noise Ratio (PSNR) values of the image stabilization images obtained by the improved and original image stabilization algorithms, as shown in Fig. 7.

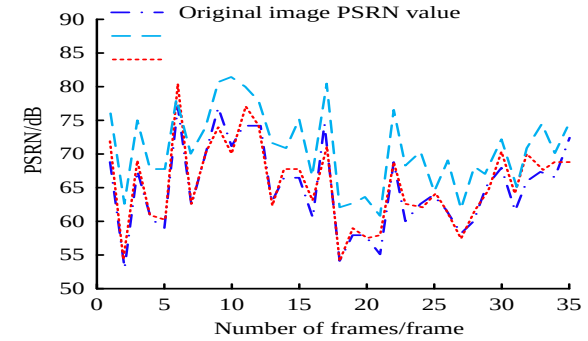

(a) PSRN value of video screen 1 and stable image

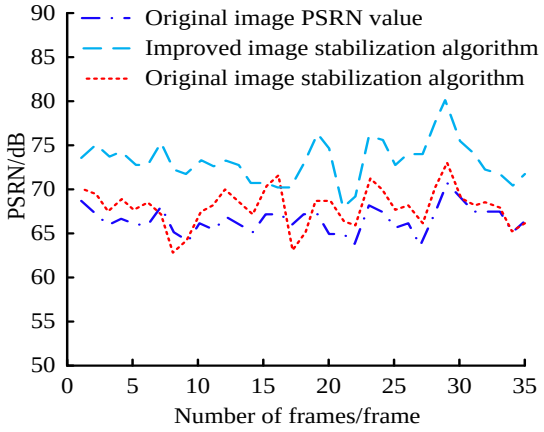

(b) PSRN value of video screen 2 and stable image

Fig. 7. Comparison of image stabilization algorithm results.

Fig. 7(a) shows the comparison of the PSNR values of the stabilized image of Video 1. The PSNR values of the improved stabilized image algorithm intersected with the PSNR values of the other two stabilized images, but overall they were still significantly better than the PSNR values of the other two stabilized images. The PSNR values of the improved stabilized image algorithm were up to 82dB and

down to 60dB, the PSNR values of the original image were up to 77dB and down to 52dB, and the PSNR values of the original stabilized image were up to 80dB and down to 54dB. Fig. 7(b) shows the comparison of the PSNR values of the stabilized image of Video 2. The improved stabilized image algorithm had significantly higher PSNR values than the other two stabilized images. In frame 16, the original stabilized image algorithm had a PSNR value of 71dB, which was higher than the improved stabilized image algorithm's 70dB. In the other frame numbers, the improved stabilized image algorithm had a PSNR value that was significantly higher than the original stabilized image, indicating a significant advantage. After confirming the effectiveness of the research in improving the image stabilization algorithm, the study compared the detection results of the Drosophila visual neural network collision detection algorithm with the improved Drosophila visual neural network algorithm, as shown in Fig. 8.

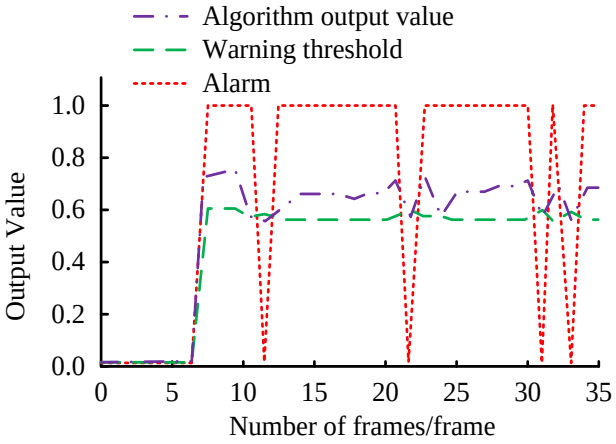

(a) Collision warning detection curve without improved algorithm

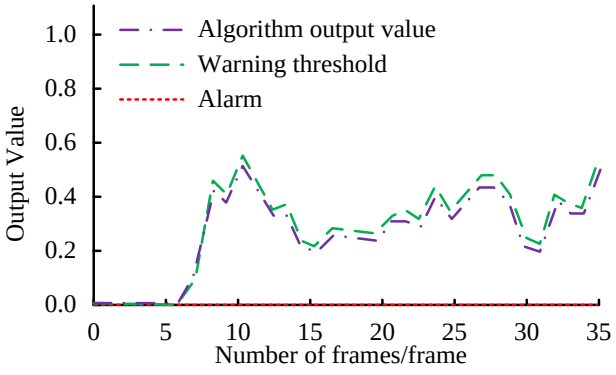

(b) Improved Algorithm for Collision Warning Detection Curve

Fig. 8. Collision warning detection results of video screen 1.

Fig. 8(a) shows the collision warning detection results of the unimproved algorithm. Only at frames 12, 22, 31, and 34, the output value of the algorithm was less than the alarm threshold, and in the remaining frames, the output value of the algorithm was higher than the threshold, requiring an alarm. Fig. 8(b) shows the collision detection probability results of the improved algorithm. The output value of the algorithm was always below the warning threshold, and there was no need to alarm. Based on the video content, a moving vehicle appears in frame 7 of the video. Afterwards, the moving vehicle began to move away from the camera, and a safe distance was maintained between the moving vehicle and the camera without warning. Therefore, the false alarm situation of the unimproved algorithm was relatively serious, while the improved algorithm did not show any false alarms. The detection results of the two algorithms in video 2 are shown in Fig. 9.

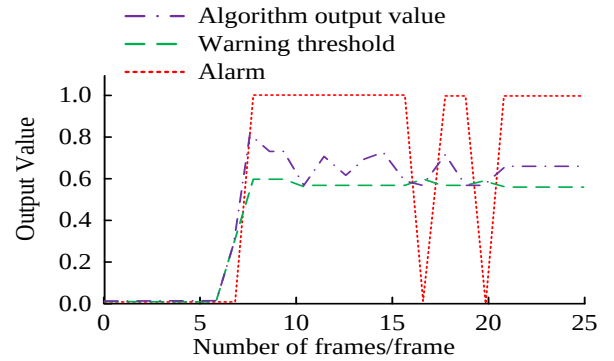

(a) The collision warning detection effect of the original algorithm

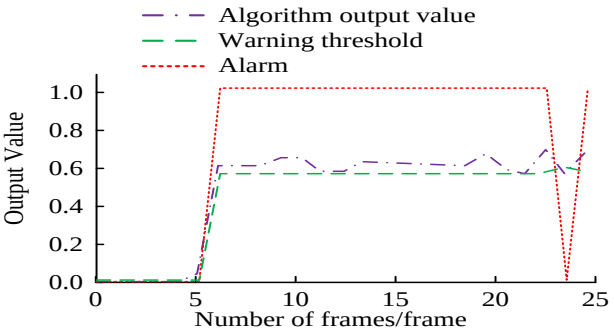

(b) Improved Algorithm for Collision Warning Detection

Fig. 9. Collision warning detection results of video screen 2.

Fig. 9(a) shows the collision warning detection results of the unimproved algorithm. Starting from frame 6, the alarm threshold started to rise. At frame 8, when the algorithm output value exceeded the alarm threshold, the algorithm started to alarm. At frames 17 and 20, when the algorithm output value was lower than the alarm threshold, the alarm was canceled. Fig. 9(b) shows the collision warning detection results of the improved algorithm. Starting from frame 5, the alarm threshold rose to around 0.6 and stabilizes. At this point, the algorithm output value was higher than the alarm threshold, and the algorithm remains in an alarm state. Based on the content of video 2, the moving vehicles were gradually approaching the camera, and the predicted results of this settlement method were more in line with the actual results.

B. Collision Warning Effect

Before verifying the collision warning effect, the research first verified the feasibility of target calibration and tracking algorithms to obtain the motion curve of moving targets in the video sequence. The results are shown in Fig. 10.

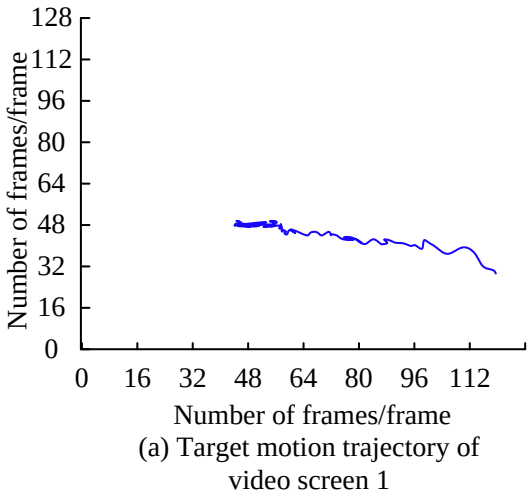

(a) Target motion trajectory of video screen 1

(b) Target motion trajectory of video screen 2

Fig. 10. Motion curves of vehicles with targets in two different types of videos.

Fig. 10(a) shows the tracking curve of the moving target in video 1. In video 1, there was only one target vehicle, and the tracking curve gradually moved from the right side towards the center of the camera's visual area, indicating that the target gradually moved away from the camera from the right side, which was consistent with the actual situation in the video. Fig. 10(b) shows the tracking curve of the moving target in video 2. There were two target vehicles in video 2. The motion curve of the first moving target gradually moved towards the center of the camera's visual area from the left, while the second vehicle hovered on the right side of the camera's visual area, which was consistent with the actual situation in the video. After extracting the target motion curve, the study compared the traditional collision warning model with the collision warning model designed in the study. The warning effect in two video scenarios is shown in Fig. 11 for video 1.

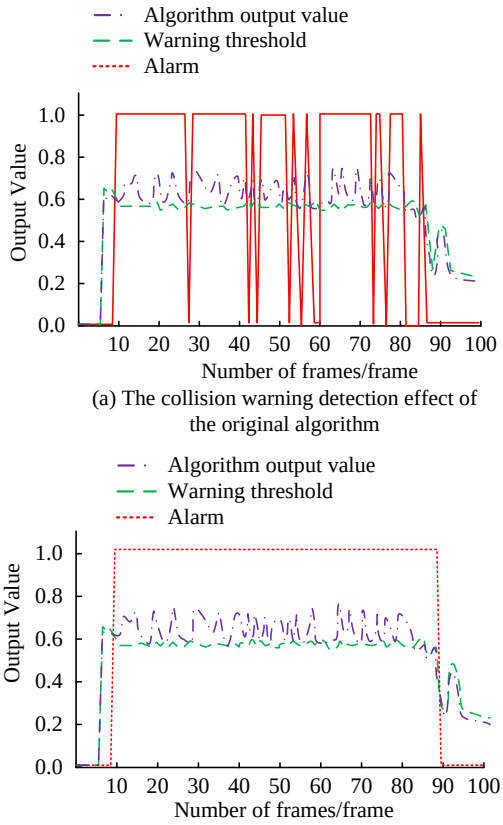

(a) The collision warning detection effect of the original algorithm

(b) Improved Algorithm for Collision Warning Detection

Fig. 11. Comparison of two algorithms for warning effects in video 1.

Fig. 11(a) shows the warning effect of the traditional collision warning algorithm. At frame 6, the moving target began to appear, and the algorithm started to alarm until frame 89. During frames 9 to 89, there were multiple occurrences of non-alarm areas, and the algorithm output values were all above the alarm threshold. Fig. 11(b) shows the collision warning effect of the research and design algorithm. From frame 9 when the moving target appeared to frame 89, the moving target left the visual area, the algorithm was in an alarm state without any missed alarms. The warning effect of Video 2 is shown in Fig. 12.

Fig. 12(a) shows the warning effect of traditional collision warning algorithms. During frames 1 to 18, the moving target appeared, and the algorithm output value and alarm threshold fluctuated. Starting from frame 22, the algorithm started to intermittently alarm, and the overall output value of the algorithm remained above the warning threshold. Fig. 12 (b) shows the collision warning effect of the research and design algorithm. The changes in the algorithm output value and warning threshold from frames 1 to 18 were consistent with traditional algorithms. Since frame 22, the research and design algorithm was always in a warning state. Based on the analysis of video content, traditional algorithms suffered from serious false positives, while research and design algorithms showed no false positives.

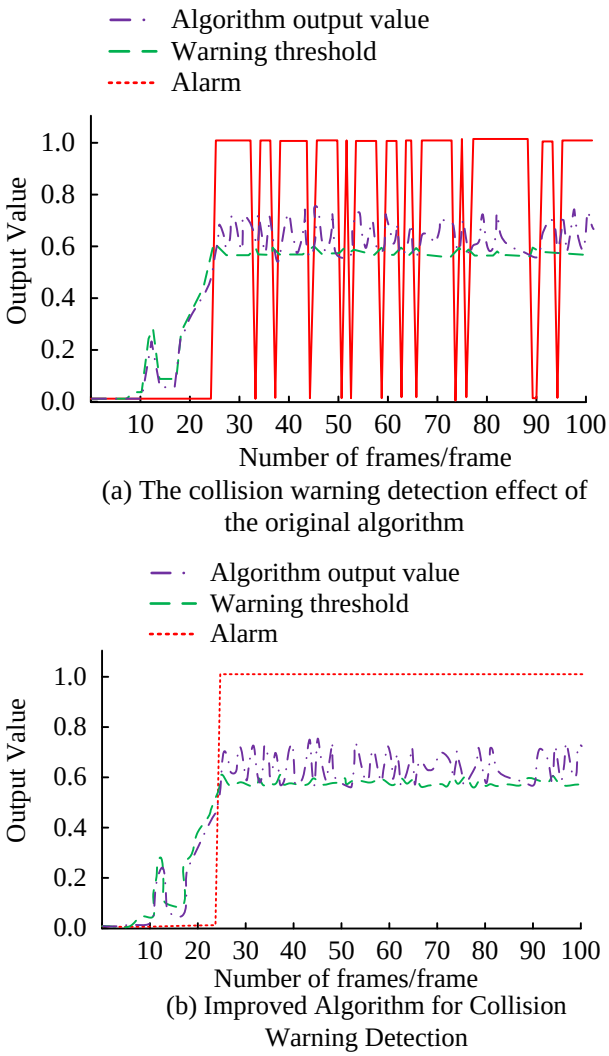

Fig. 12. Comparison of two algorithms for warning effects in video 2.

V. CONCLUSION

To increase the safety of vehicle driving and ensure the safety of drivers' lives and property, a vehicle tracking and collision warning model based on improved Drosophila vision is studied, designed, and constructed. The model adopts motion vector estimation algorithms, image stabilization algorithms, target region synthesis algorithms, target tracking algorithms, and collision warning algorithms that are improved based on traditional algorithms. The results showed that the PSNR value of the improved image stabilization algorithm was always higher than that of the original image and traditional image stabilization algorithms. The PSNR value of the improved image stabilization algorithm was highest at 82dB and lowest at 60dB, while the PSNR value of the traditional image stabilization algorithm was highest at 80dB and lowest at 54dB. The improved Drosophila visual neural network collision warning algorithm had no false positives, and the original algorithm had four false positives in video 1. The research and design of the target region synthesis algorithm can complete the task of extracting motion curves of video moving targets. The algorithm extracted the motion curves of one target in video 1 and two targets in video 2, which were consistent with the video content. The target tracking and collision warning algorithm designed in the study did not show any false positives. In the collision warning effects of Video 1 and Video 2, the original algorithm showed relatively serious false positives, while the algorithm designed in the study did not, which was consistent with the actual information in the video. The algorithm designed through research has improved the missed and false positives of the original algorithm, but the improved image stabilization algorithm has poor performance when facing multiple objectives. Subsequent research can continue to optimize the application effect of the model in multi-objective situations.

REFERENCES

[1] C. Pek, S. Manzinger, M. Koschi, and M. Althoff, "Using online verification to prevent autonomous vehicles from causing accidents," *Nat. Mach. Intell.*, vol. 2, no. 9, pp. 518–528, Sept. 2020.

[2] A. Borucka, E. Kozowski, P. Oleszczuk, and A. Widerski, "Predictive analysis of the impact of the time of day on road accidents in Poland," Open Eng., vol. 11, no. 1, pp. 142-150, Dec. 2020.

[3] W. P. Sanberg, G. Dubbelman, and P. With, "ASTEROIDS: A stixel tracking extrapolation-based relevant obstacle impact detection system," IEEE Trans. Intell. Vehicles, vol. 6, no. 4, pp. 34-46, Mar. 2020.

[4] J. Hu, Y. Zhang, and S. Rakheja, "Path planning and tracking for autonomous vehicle collision avoidance with consideration of tire-road friction coefficient," IFAC-PapersOnline, vol. 53, no. 2, pp. 15524-15529, Jul. 2020.

[5] F. Cao, and H. Jiang, "Trajectory planning and tracking control of unmanned ground vehicle leading by motion virtual leader on expressway," IET Intell. Transp. Syst., vol. 15, no. 2, pp. 187-199, Dec. 2020.

[6] X. Zhou, X. Yu, Y. Zhang, Y. Luo, and X. Peng, "Trajectory planning and tracking strategy applied to an unmanned ground vehicle in the presence of obstacles," IEEE Trans. Autom. Sci. Eng., vol. 18, no. 4, pp. 1575-1589, Aug. 2020.

[7] F. Tokuda, S. Arai, and K. Kosuge, "Convolutional neural network-based visual servoing for eye-to-hand manipulator," IEEE Access, vol. 9, no. 6, pp. 91820-91835, Jun. 2021.

[8] A. Burguera and F. Bonin-Font, "An unsupervised neural network for loop detection in underwater visual SLAM," J. Intell. Robot. Syst., vol. 100, no. 3/4, pp. 1157-1177, Aug. 2020.

[9] Q. Gu, J. Su, and L. Yuan, "Visual affordance detection using an efficient attention convolutional neural network," Neurocomputing, vol. 440, no. 14, pp. 36-44, Jun. 2021.

[10] Q. Fu, C. Hu, J. Peng, F. C. Rind, and S. Yue, "A robust collision perception visual neural network with specific selectivity to darker objects," IEEE Trans. Cybern., vol. 50, no. 12 pp. 5074-5088, Dec. 2020.

[11] J. Tao, C. Yang, and C. Xu, "Estimation algorithm of incident sources' stokes parameters and 2 ℎ DOAs based on reduced mutual coupling vector sensor," Radio Ence, vol. 54, no. 7/8, pp. 770-784, Aug. 2019.

[12] W. Choi, I. Y. Song, and V. Shin, "Two-stage algorithm for estimation of nonlinear functions of state vector in linear Gaussian continuous dynamical systems," J. Comput. Syst. Sci. Int., vol. 58. no. 6, pp. 869-882, Feb. 2019.

[13] M. D. Hua, J. Trumpf, T. Hamel, R. Mahony, and P. Morin, "Feature-based recursive observer design for homography estimation and its application to image stabilization: Feature-based Recursive Observer Design for Homography Estimation," Asian J. Control, vol. 21, no. 4, pp. 1443-1458, Jan. 2019.

[14] T. Rasal, T. Veerakumar, B. N. Subudhi, and S. Esakkirajan, "Mixed poisson gaussian noise reduction in fluorescence microscopy images using modified structure of wavelet transform," Image Process., IET, vol. 15, no. 7, pp. 1383-1398, Dec. 2020.

[15] Z. Chen, "Research on internet security situation awareness prediction technology based on improved RBF neural network algorithm," J. Comput. Cogn. Eng., vol. 1, no. 3, pp. 103-108, Mar. 2022.

[16] A. N. Sharkawy, P. N. Koustoumpardis, and N. Aspragathos, "Neural network design for manipulator collision detection based only on the joint position sensors," Robotica, vol. 38, no. 10, pp. 1737-1755, Jun. 2020.

[17] X. Yang, S. Zhu, D. Zhou, and Y. Zhang, "An improved target tracking algorithm based on spatio-temporal context under occlusions," Multidimension. Syst. Signal Process., vol. 31, no. 1, pp. 329-344, Jun. 2020.

[18] X. Fang and L. Chen, "Noise-aware manoeuvring target tracking algorithm in wireless sensor networks by a novel adaptive cubature Kalman filter,". IET Radar, Sonar Navig., vol. 14, no. 11, pp. 1795-1802, Sept. 2020.